Supporting Information

Construction of an In-BDC MOF Artificial Interface Layer on Zinc Metal Anode for Ultra-Long Stability Zinc-Ion Capacitors

Yuxue Deng[a], Nuo Cheng[a], Hongfang Ma[a], Pingfan Zhou[a], Peng Huang[a], Zhenming Xu[a], Laifa Shen[a], Xiaogang Zhang[a]*, Hao Tong[a]**

[a] Jiangsu Key Laboratory of Electrochemical Energy-Storage Technologies College of Materials Science and Technology Nanjing University of Aeronautics and Astronautics No. 29 Yudao Street, Nanjing 210016, P. R. China

E-mail: tongh@nuaa.edu.cn (Hao Tong), lfshen@nuaa.edu.cn (Laifa Shen), axgzhang@nuaa.edu.cn (Xiaogang Zhang)

*Corresponding author.

Experimental Section

Preparation of Electrode Materials

The synthesis of In-BDC MOF was carried out following a procedure adapted from literature[28]. Indium nitrate hydrate (3 g), 1,4-benzenedicarboxylic acid (1.661 g), N,N-dimethylformamide (100 mL), and sodium acetate aqueous solution (0.5 mL) were mixed and stirred for 30 min. The resulting solution was then heated to 120 °C and maintained at this temperature for 2 h. After cooling to room temperature, the white precipitate was washed three times with anhydrous ethanol and dried overnight under vacuum at 60 °C.

Zinc foil with a thickness of 100 μm was polished with sandpaper, cut into circular discs with a diameter of 12 mm, and cleaned three times with anhydrous ethanol for subsequent use. In-BDC MOF powder, acetylene black, and poly(vinylidene fluoride) (PVDF) were thoroughly mixed in a mass ratio of 8:1:1. N-Methyl-2-pyrrolidone (NMP) was added as the solvent to form a homogeneous slurry, which was then uniformly coated onto the zinc foil. The coated electrode was dried in a vacuum oven at 60 °C for 12 h to obtain the In-BDC@Zn material.

Preparation of Cathode Materials

Activated carbon (AC), acetylene black, and PVDF were uniformly mixed in a mass ratio of 8:1:1. NMP was used as the solvent to form a homogeneous slurry, which was then coated onto carbon cloth. The coated electrode was dried in a vacuum oven at 60 °C for 12 h to obtain the AC cathode.

Materials Characterization

The crystal structures of the obtained samples were determined by X-ray diffraction (XRD) analysis using a Bruker AXS-D8 powder X-ray diffractometer. Fourier transform infrared (FTIR) spectra were recorded on a PerkinElmer spectrometer over the range of 300-4000 cm^{-1} to investigate the structural features and identify characteristic functional groups. The morphology and elemental distribution of the samples were characterized using a Hitachi S-4800 scanning electron microscope (SEM) equipped with an energy-dispersive X-ray spectrometer (EDS). Raman spectra were acquired with a LabRAM HR Evolution Raman spectrometer to further confirm the material composition. Nitrogen adsorption-desorption isotherms were measured at 77 K on a Micromeritics ASAP-2020HD88 surface area and porosity analyzer to evaluate specific surface area and pore size distribution. X-ray photoelectron spectroscopy (XPS) was performed on a PHI550 spectrometer with an Al-Kα radiation source (1486.6 eV) to analyze surface elemental composition and chemical states. The wettability of the electrodes toward the electrolyte was evaluated using a contact angle goniometer.

Electrochemical Measurements

Electrochemical Performance Testing

A three-electrode configuration was assembled in 1 M Na_2SO_4 aqueous electrolyte, using a saturated calomel electrode (Hg/Hg_2Cl_2) as the reference electrode, a platinum foil as the counter electrode, and either In-BDC@Zn or bare Zn as the working electrode. Corrosion resistance was evaluated by potentiodynamic polarization measurements conducted over a potential range from -0.8 to -1.4 V at a scan rate of 1

mV s^{-1}. Linear sweep voltammetry (LSV) tests were performed within a potential window of -2.0 to -1.0 V at a scan rate of 1 mV s^{-1}.

Zinc-ion hybrid capacitors were employed for cyclic voltammetry (CV) and electrochemical impedance spectroscopy (EIS) measurements. CV tests were carried out in a voltage range of 0.2-1.8 V at scan rates of 5, 10, 20, 50, and 100 mV s^{-1}. EIS measurements were conducted over a frequency range from 0.01 to 10^6 Hz.

Zinc-ion symmetric cells were used to determine the Zn^{2+} transference number. The Zn^{2+} transference number ($T_{Zn^{2+}}$) was calculated according to Equation (1):

$$T_{Zn^{2+}} = \frac{I_s(\Delta V - I_0 R_0)}{I_0(\Delta V - I_s R_s)} \#\ (1)$$

Here, ΔV represents the applied polarization voltage, I_0 is the initial current, I_s corresponds to the steady-state current, R_0 denotes the interfacial resistance before polarization, and R_s is the interfacial resistance after reaching the steady state.

Temperature-dependent electrochemical impedance measurements were carried out in the temperature range of 40-60 °C with an interval of 5 °C. The Zn^{2+} desolvation energy (E_a) of the electrodes was subsequently calculated using the Arrhenius equation:

$$\frac{1}{R_{ct}} = A exp\left(-\frac{E_a}{RT}\right) \#\ (2)$$

Here, R_{ct} represents the charge-transfer resistance, A is the Arrhenius constant, R is the universal gas constant, and T denotes the absolute temperature.

The energy density (E_s) and power density (P_s) of the zinc-ion hybrid capacitor were calculated from the galvanostatic charge-discharge (GCD) profiles according to the following equations:

$$C_{cell} = \frac{I\Delta t}{mV} \#\ (3)$$

$$E_s = \frac{0.5 C_{cell} V^2}{3.6} \#\ (4)$$

$$P_s = \frac{3600 E_s}{\Delta t} \#\ (5)$$

Here, C_{cell} denotes the specific capacitance of the device, I is the discharge current, Δt represents the discharge time, m corresponds to the mass loading of the active material in the cathode, and V is the effective discharge voltage window.

Density Functional Theory (DFT) Calculations

Spin-polarized density functional theory (DFT) calculations[1,2] were performed using a plane-wave basis set within the projector augmented-wave (PAW) method, as implemented in the Vienna *ab initio* simulation package (VASP)[3,4] The exchange–correlation interactions were treated using the Perdew-Burke-Ernzerhof (PBE) functional within the generalized gradient approximation (GGA) framework[5]. To eliminate interactions between periodic images, a vacuum layer of approximately 15 Å was introduced along the surface normal direction. The plane-wave energy cutoff was set to 450 eV. Brillouin zone integrations were carried out using a Γ-centered 1 × 1 × 1 Monkhorst-Pack *k*-point mesh. All structures were fully relaxed until the total energy convergence criterion reached 1×10^{-5} eV, and the maximum residual force on each atom was less than 0.03 eV $Å^{-1}$. The adsorption energy (E_{ads}) was defined as: $E_{ads} = E_{*M} - E_{*} - E_{M}$. where E_{*M} is the total energy of the substrate with the adsorbed species *M*, E_{*} is the energy of the clean substrate, and E_M represents the energy of an isolated *M* species in vacuum. Visualization of crystal structures and charge density distributions was performed using the VESTA software.

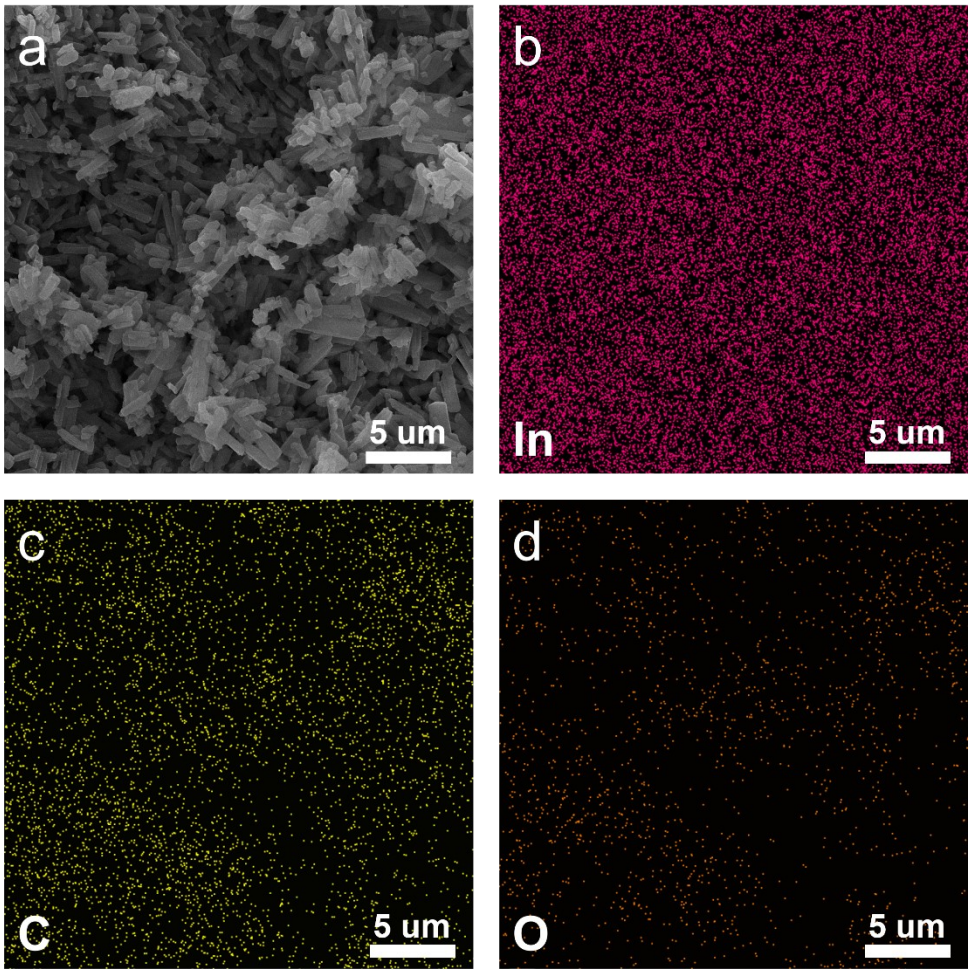

106

107 Figure S1. (a-d) EDS mapping diagram of In-MOF powder

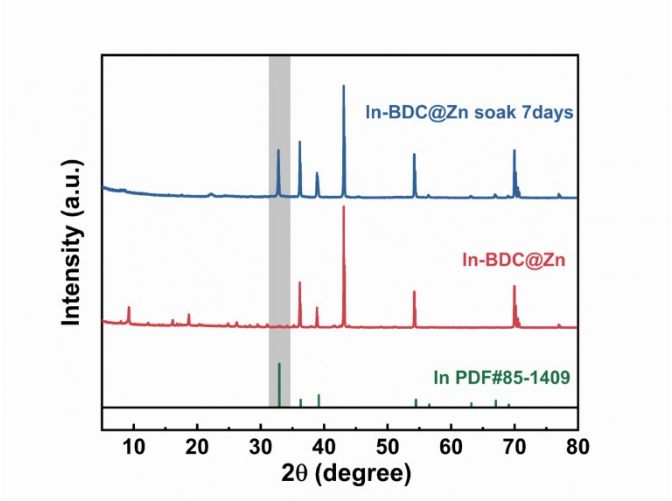

108

109 Figure S2. Comparison of XRD patterns of In-BDC@Zn before and after 7 days of

110 immersion

111

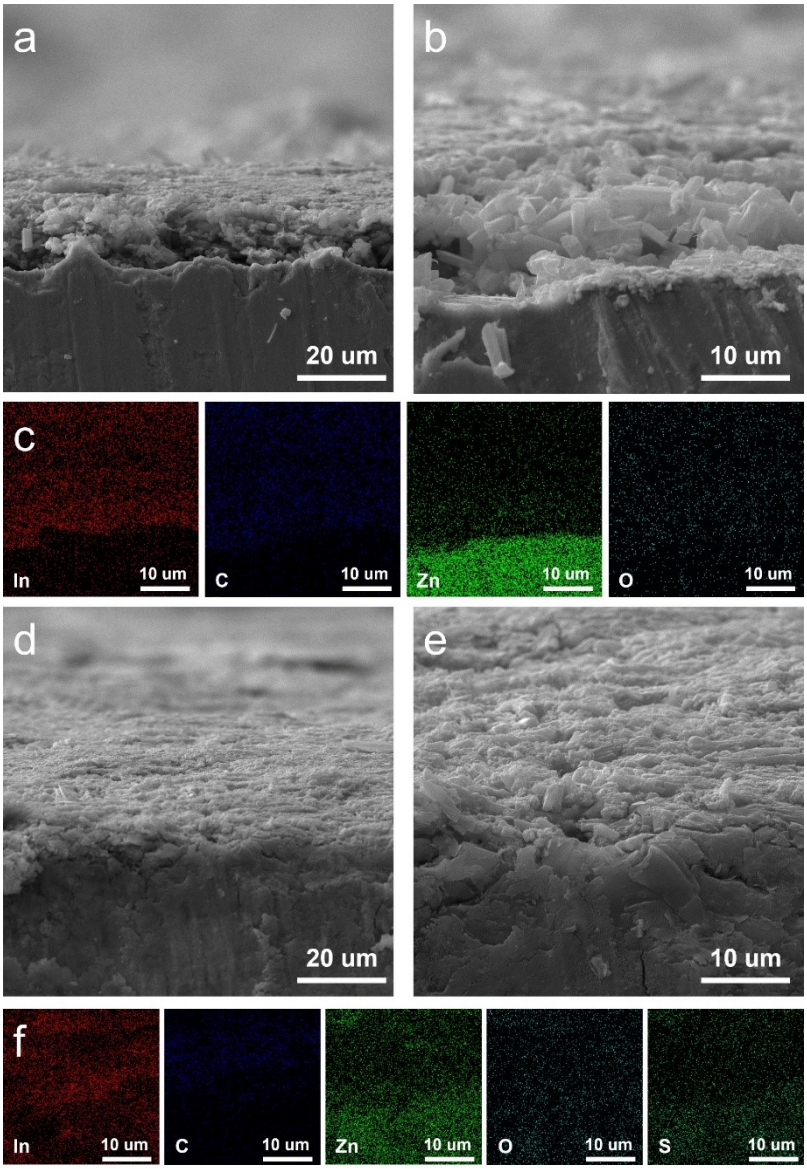

Figure S3. (a-b) Cross-sectional SEM images of In-BDC@Zn; (c) Cross-sectional EDS-mapping image of In-BDC@Zn; (d-e) Cross-sectional SEM images of In-BDC@Zn after 7 days of immersion; (f) Cross-sectional EDS-mapping image of In-BDC@Zn after 7 days of immersion

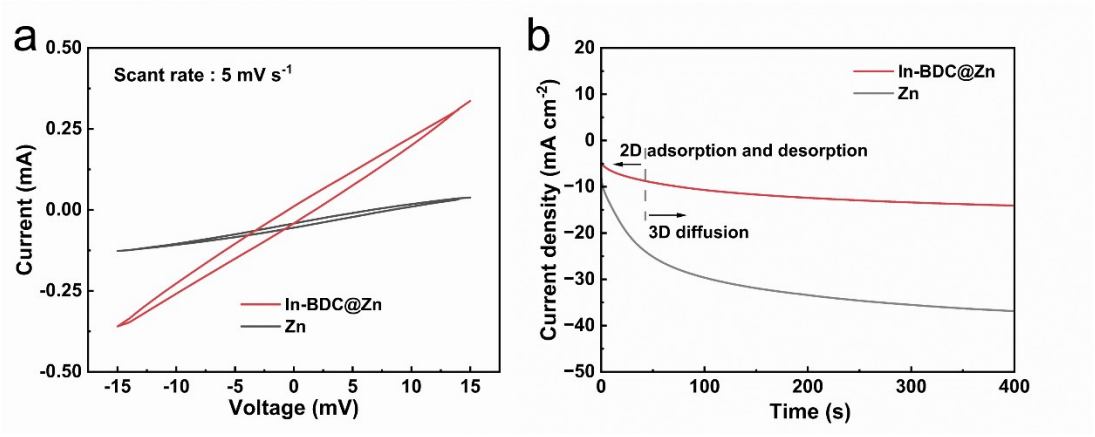

Figure S4. (a) Comparison of CV curves for In-BDC@Zn//In-BDC@Zn and Zn//Zn symmetric cells at a scan rate of 5 mV s^{-1}; (b) Chronoamperometry curve under constant voltage polarization at -150 mV

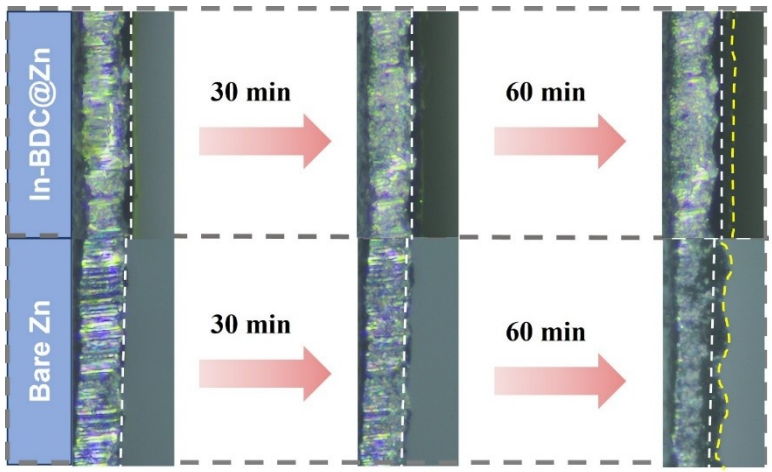

Figure S5. In situ optical microscopy images of the electroplating process for In-BDC@Zn and bare Zn electrodes at a current density of 10 mA cm^{-2}

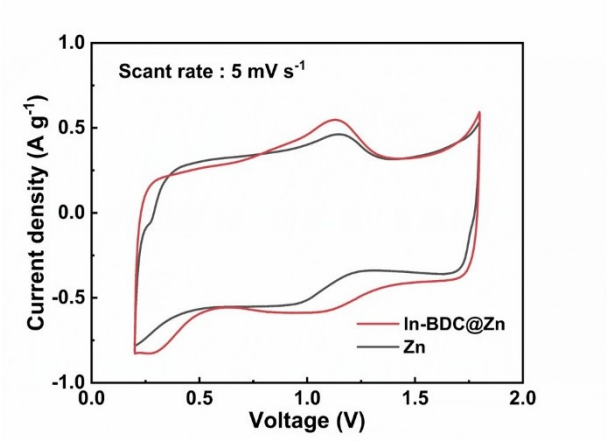

Figure S6. CV curves of In-BDC@Zn and bare Zn at 5 mV s^{-1}

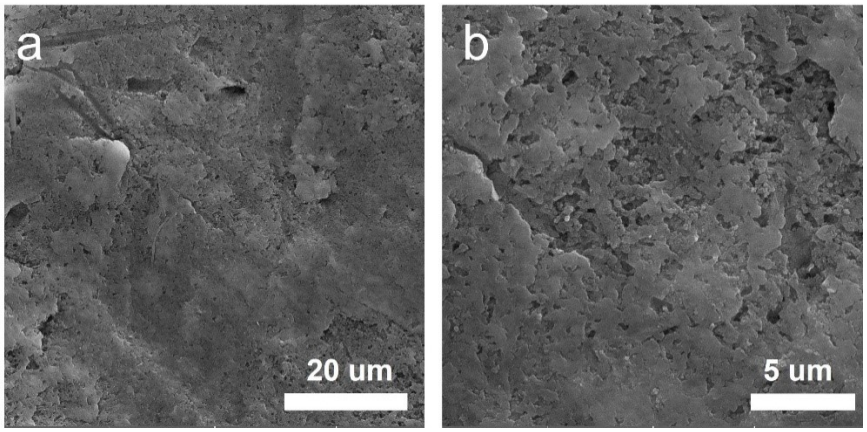

Figure S7. SEM images of the In-BDC@Zn electrode after cycling at 20 mA cm^{-2} and 0.5 mAh cm^{-2} for 1000 h

References

[1] P. Hohenberg, W. Kohn, Inhomogeneous electron gas, Phys. Rev. 136 (1964) B864.

[2] W. Kohn, L. J. Sham, Self-consistent equations including exchange and correlation effects, Phys. Rev. 140 (1965) A1133

[3] G. Kresse, J. Furthmüller, Efficient iterative schemes for ab initio total-energy calculations using a plane-wave basis set, Phys. Rev. B 54 (1996) 11169.

[4] P. E. Blöchl, Projector augmented-wave method, Phys. Rev. B 50 (1994) 17953.

[5] J. P. Perdew, K. Burke, M. Ernzerhof. Generalized gradient approximation made simple, Phys. Rev. Lett. 77 (1996) 3865.